Membrane Water Treatment, *Vol. 6, No. 6 (2015) 451-476*
DOI: http://dx.doi.org/10.12989/mwt.2015.6.6.451

Optimization of three small-scale solar membrane distillation desalination systems

Hsuan Chang [*], Chen-Yu Hung [a], Cheng-Liang Chang [b], Tung-Wen Cheng [c] and Chii-Dong Ho [d]

Department of Chemical and Materials Engineering, Tamkang University, 151 Yingzhuan Rd., Tamsui Dist., New Taipei City, Taiwan (R.O.C.)

(*Received January 17, 2015, Revised October 23, 2015, Accepted October 24, 2015*)

Abstract. Membrane distillation (MD), which can utilize low-grade thermal energy, has been extensively studied for desalination. By incorporating solar thermal energy, the solar membrane distillation desalination system (SMDDS) is a potential technology for resolving the energy and water resource problems. Small-scale SMDDS (s-SMDDS) is an attractive and viable option for the production of fresh water for small communities in remote arid areas. The minimum-cost design and operation of s-SMDDS are determined by a systematic method, which involves a pseudo steady state approach for equipment sizing and the dynamic optimization using overall system mathematical models. The s-SMDDS employing three MD configurations, including the air gap (AGMD), direct contact (DCMD) and vacuum (VMD) types, are optimized. The membrane area of each system is 11.5 m^2. The AGMD system operated for 500 kg/day water production rate gives the lowest unit cost of \$5.92/m^3. The performance ratio and recovery ratio are 0.85 and 4.07%, respectively. For the commercial membrane employed in this study, the increase of membrane mass transfer coefficient up to two times is beneficial for cost reduction and the reduction of membrane heat transfer coefficient only affects the cost of the DCMD system.

Keywords: solar energy; desalination; membrane distillation; optimization; dynamic modeling

1. Introduction

Membrane distillation (MD) is a thermal-driven membrane separation process, in which only vapor molecules are transported through porous hydrophobic membranes. The driving force is the vapor pressure difference between the hot liquid feed side and the cold permeate side of the membrane. Latest comprehensive review of various aspects of MD technology, including fundamental concept, membrane configuration, membrane characteristics, membrane modules, applications, heat and mass transfer mechanisms, thermal efficiency and energy consumption, fouling as well as the effects of operating parameters are referred to Alkhudhiri *et al*. (2012) and

*Corresponding author, Professor, E-mail: nhchang@mail.tku.edu.tw
[a] Mater Student, E-mail: tony94m6@hotmail.com
[b] Ph.D., E-mail: chlchang@mail.tku.edu.tw
[c] Ph.D., E-mail: twcheng@mail.tku.edu.tw
[d] Ph.D., E-mail: cdho@mail.tku.edu.tw

Camacho *et al*. (2013). MD has many applications, such as desalination, heavy metal removal from waste water and aqueous solution concentration in food industry. Desalination is the most studied MD application. The advantages of MD over other desalination processes include less sensitivity to feed concentration, ability to use low temperature heat, ability to use relatively cheap and robust membranes, high product quality, high system compactness and high fouling resistance (Camacho *et al*. 2013).

Being capable of directly utilizing renewable solar thermal energy, the solar membrane distillation desalination system (SMDDS) has evolved as a promising technology for alleviating the energy and water resource problems simultaneously. Small-scale SMDDS (s-SMDDS) is an attractive and viable option for the production of fresh water for small communities in remote arid areas. The EU-funded SMADES project (PV and thermally driven small-scale, stand-alone desalination systems with very low maintenance needs (Fath *et al*. 2006) and MEDESOL project (seawater desalination by innovative solar-powered membrane distillation system) have both developed and investigated s-SMDDS (MEDESOL project web site).

Qtaishat and Banat (2013) reviewed the research efforts of coupling MD modules with various solar energy systems, including flat plate collectors, vacuum collectors, solar ponds, solar stills and parabolic troughs. The MD modules employed for SMDDS include hollow fiber module, spiral-wound module with heat recovery and compact flat plate module. The MD configurations adopted for SMDDS include direct contact (DCMD), air gap (AGMD), liquid gap (LGMD) and vacuum (VMD) types. The small and lab scale SMDDS tested have shown that MD process is suitable to operate in conjunction with solar energy for small capacities. The few economic studies showed that the pure water production costs of SMDDS are much higher than other desalination technologies. Banat and Jwaied (2008) estimated the costs of two s-SMDDS, which employ spiral-wound LGMD modules, developed in the SMADES project to be \$15/m^3 and \$18/m^3 for a compact unit (specified by 100 L/day capacity and 10 m^2 membrane area) and a large unit (specified by 500 L/day capacity and 40 m^2 membrane area), respectively. In the MEDESOL project, the water production costs of three small stand-alone solar systems of different heat recovery configurations were analyzed (MEDESOL project 2006). The systems employed the flat plate AGMD module (of 2.8 m^2 membrane area) developed and manufactured by the Swedish company Scarab AB. With specified operation conditions and solar collector area, the production costs estimated are \$15.67/m^3 for brackish water and \$31.34/m^3 for sea water. Recently, Saffarini *et al*. (2012) evaluated the water production costs of three solar-powered MD desalination systems that employ DCMD, AGMD and VMD configurations but with the same specified membrane area of 7 m^2 and recovery ratio of 4.4%. The water production costs of the systems using DCMD, AGMD and VMD modules are \$12.7/m^3, \$18.26/m^3 and \$16.02/m^3, respectively. For the system using AGMD module, Saffarini *et al*. (2012) also examined the effects of design and operation parameters and concluded that these parameters can significantly affect the water production cost.

Although not specifically commenting on SMDDS, Khayet and Matsuura (2011) pointed out that the commercial application of MD technology is hindered by energy efficiency and economics. Summers *et al*. (2012) emphasized that most research on MD has focused on maximizing membrane flux as opposed to minimizing energy consumption and cost. However, in MD systems, membrane flux is not only determined by the membrane characteristics, but also highly dependent on system configuration, membrane area, energy input, and heat recovery from hot fluid and condensing vapor. Furthermore, in a complete system, the highest membrane flux operation may not lead to the best use of energy or the lowest cost. It is imperative that the minimum-cost SMDDS designs, which should be obtained via overall system optimization, be identified to justify

the economic feasibility of SMDDS. In addition, the significance of enhancing membrane characteristics, which is the focus of many researches, should be examined from the overall system cost reduction point of view.

The aim of this study is to determine and compare the minimum water production costs of s-SMDDS employing three MD configurations by a systematic method. The MD configurations investigated include the AGMD, DCMD and VMD. In this paper, rigorous mathematical models for the equipment units of the systems, including solar collector, thermal storage tank, heat exchanger and membrane distillation module, are developed and integrated for the simulation of the overall systems. The design and operation conditions of the s-SMDDS are then determined via dynamic optimization. The equipment sizes of the s-SMDDS, which are operated with unsteady solar radiation, are determined by a pseudo steady state approach. With the simulation models, the effects of membrane characteristics on the water production cost are analyzed by varying the mass and heat transfer resistances of the membrane.

2. Systems

In this study, the flowsheets of the s-SMDDS using AGMD, DCMD and VMD modules, are developed, respectively. In an AGMD module, the feed side of the As depicted in Fig. 1, the AGMD system includes a solar collector, a thermal storage tank, a heat exchanger, the AGMD module and four pumps. Instead of PV (photovoltaic) modules, the electricity needed comes from an electric grid. The solar thermal energy is absorbed and transferred to the thermal storage tank by the fluid circulation in loop 1. The thermal energy is further transferred via loop 2 fluid circulation to the heat exchanger, where the feed stream of the AGMD module is heated. Inside the AGMD module, the sensible heat of hot stream is recovered by the cold stream flows in countercurrent mode (Meindersma *et al*. 2005). Around the AGMD module, both hot side and cold side heat recovery configurations are included in the flowsheet. In the hot side recovery configuration, part of the hot side outlet stream of the MD module, the stream S8, is sent to the heat exchanger for further heating. In the cold side configuration, part of the cold side outlet stream of the MD module, the stream S9, which has been heated in the module by the hot stream, is sent to the heat exchanger for further heating. These two heat recovery configurations have been proposed and analyzed in MEDESOL project (2006).

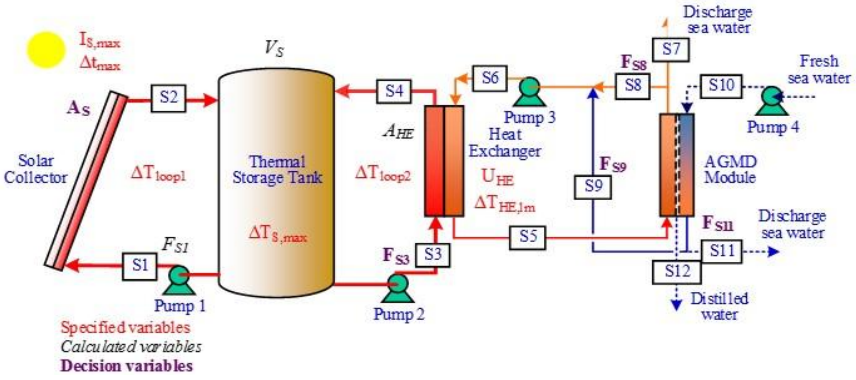

Fig. 1 Solar air gap membrane distillation desalination system

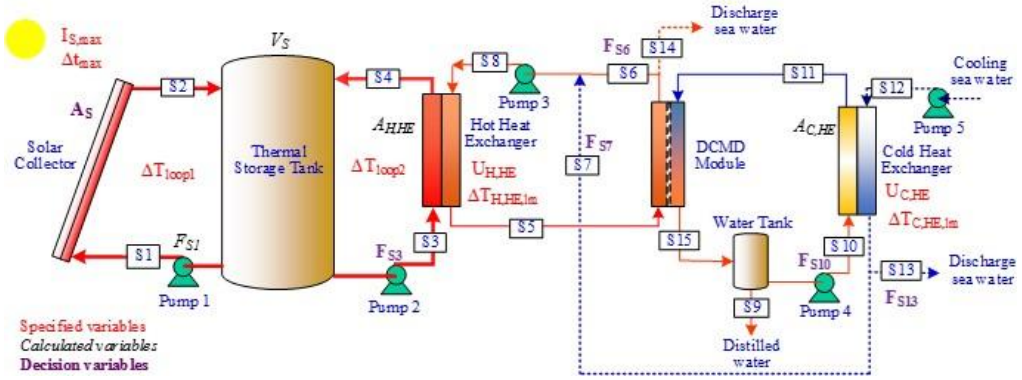

Fig. 2 Solar direct contact membrane distillation desalination system

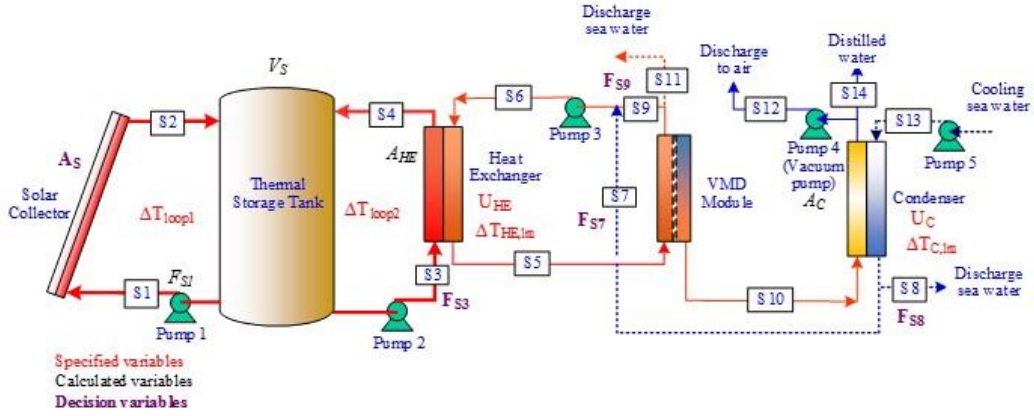

Fig. 3 Solar vacuum membrane distillation desalination system

The system using DCMD is shown in Fig. 2. Compared to the AGMD system, the major difference is that one more heat exchanger at the cold-end of the flowsheet is needed. The cold heat exchanger uses cold fresh sea water to cool the cold side distilled water of the DCMD module. Same as the AGMD system, around the DCMD, both the hot side and cold side heat recovery configurations are included. The streams S6 and S7 are sent to the hot heat exchanger for further heating.

The system using VMD is shown in Fig. 3. Compared to the DCMD system, the cold heat exchanger is replaced by a condenser, which is used to condense the permeate side vapor from the DCMD module. The vacuum pump which creates the low pressure in the permeate side of the membrane module is located downstream of the condenser. The hot side and cold side heat recovery configurations are also included and the streams sent to the hot heat exchanger are S9 and S7.

3. Modeling

Same as other thermal and chemical processes, the individual equipment of SMDDS can be simulated by developing models from the fundamental principles. Furthermore, one can build the

models on many commercial process simulation platforms, which enable easy study of the design alternatives of the equipment units and the overall flowsheet. Chang *et al*. have reported the model development and the flowsheet analysis for the SMDDS using DCMD and AGMD modules on Aspen Plus® and Aspen Custom Modeler® platforms (Chang *et al*. 2009, 2010, 2012, 2013).

One-dimensional (1-D) models are developed for individual equipment units of the SMDDS. Considering the differences in time constants of the equipment units, not all the dynamics of the equipment units are included in the models. For the solar collector, thermal storage tank and heat exchanger, only the thermal dynamics are considered. For the MD module, the transients of both mass flow and energy flow are ignored.

For the solar collector, the energy balance taking into account the energy flows associated with mass convection and solar radiation with the collector efficiency (η_{SC}) is

$$\frac{\partial T_{f,SC}}{\partial t} = -L_{SC}\frac{m_{f,SC}}{M_{f,SC}}\frac{\partial T_{f,SC}}{\partial x} + \frac{A_{SC}I(t)\eta_{SC}}{M_{f,SC}Cp} \tag{1}$$

For the thermal storage tank, because the size is small for the s-SMDDS, the ideal temperature stratification inside the tank may not be achievable. A conservative approach is taken in this study. The hot and cold inlet streams enter the tank concurrently. The temperature variation in the thermal storage tank with a circulation flow rate of $m_{f,ST}$ and the inlet stream which is the combination of S2 and S4 can be determined from the energy balance as

$$\frac{\partial T_{f,ST}}{\partial t} = -H_{ST}\frac{m_{f,ST}}{M_{f,ST}}\frac{\partial T_{f,ST}}{\partial x} \tag{2}$$

In the counter-current flow heat exchanger, the hot fluid comes from the thermal storage tank and the cold fluid comes from the MD module. The energy balances for both fluids, considering the energy flow of mass convection and the heat transfer between both fluids, are given as

$$\frac{dT_{f,HE,HL}}{dt} = L_{HE}\frac{m_{f,HE,HL}}{M_{f,HE,HL}}\frac{\partial T_{f,HE,HL}}{\partial x} - \frac{A_{HE}U_{HE}}{M_{f,HE,HL}Cp}\left(T_{f,HE,HL} - T_{f,HE,CL}\right) \tag{3}$$

$$\frac{dT_{f,HE,CL}}{dt} = -L_{HE}\frac{m_{f,HE,CL}}{M_{f,HE,CL}}\frac{\partial T_{f,HE,CL}}{\partial x} + \frac{A_{HE}U_{HE}}{M_{f,HE,CL}Cp}\left(T_{f,HE,HL} - T_{f,HE,CL}\right) \tag{4}$$

For the MD modules, a steady state 1-D model considering the heat and mass transfers in each layer and at the interface between layers. The mass and heat transfer inside the AGMD, DCMD and VMD modules are illustrated in Fig. 4. The differences among these configurations lie in the permeate side. For the AGMD, DCMD and VMD modules, the water vapor penetrates the hydrophobic membrane is condensed at the cooling plate, the cold liquid-membrane interface and the downstream condenser, respectively. In the following, the mathematic model of AGMD module is presented. The mass balance equations of the hot fluid and the condensing liquid can be written as

$$\frac{dm_{f,MD,HL}}{dx} = -N_{mem}\,Mw_w L_{MD} \tag{5}$$

$$\frac{\mathrm{dm_{f,MD,CONL}}}{\mathrm{dx}} = -\mathrm{N_{ag}\,Mw_w\,L_{MD}} \tag{6}$$

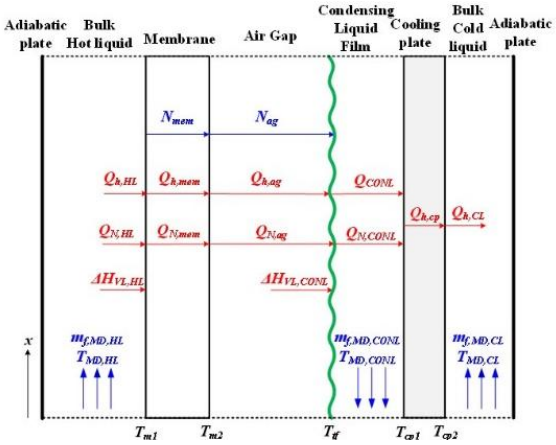

(a) AGMD

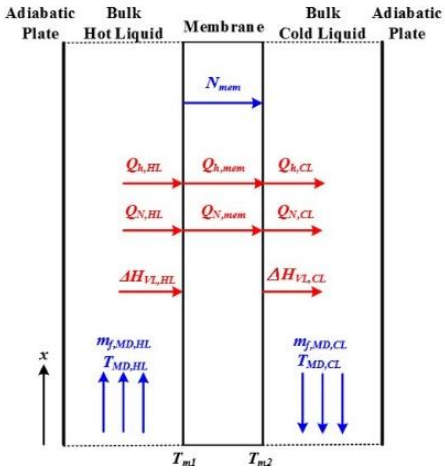

(b) DCMD

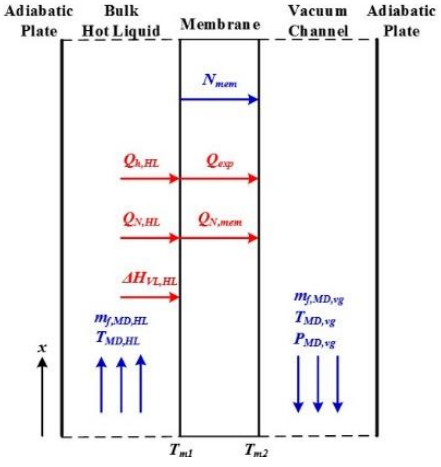

(c) VMD

Fig. 4 Heat and mass transfer inside membrane distillation modules

At the interface between membrane and air gap, the fluxes are equal

$$N_{mem} = N_{ag} \tag{7}$$

The mass fluxes are determined by the effective mass transfer coefficients and the pressure difference driving forces in the membrane and air gap layers.

$$N_{mem} = \frac{k_{mem}}{R\bar{T}_{mem}}(P_{sat,w,m1} - P_{w,m2}) \tag{8}$$

$$N_{ag} = \frac{k_{ag}P_{ag}^{T}}{R\bar{T}_{ag}P_{a,lm}}(P_{w,m2} - P_{sat,w,lf}) \tag{9}$$

For the mass transfer in the membrane, Kundsen diffusion and molecular diffusion are taken into account (Ding *et al*. 2003). For the air gap, only molecular diffusion is considered.

$$k_{mem} = \frac{\varepsilon}{\tau}\left[\frac{1}{1/D_K + y_{air,lm}/D_m}\right]\frac{1}{\delta_{mem}} \tag{10}$$

$$k_{ag} = \frac{D_m}{\delta_{ag}} \tag{11}$$

The energy balances for the hot and cold fluid channels, in addition to the energy flow of mass convection, the convective heat transfer and the sensible heat effect associated with the mass transfer across the boundaries are taken into account.

$$\frac{\partial T_{f,MD,HL}}{\partial t} = -L_{MD}\left[\frac{m_{f,MD,HL}}{M_{f,MD,HL}}\frac{\partial T_{f,MD,HL}}{\partial x} + \frac{W_{mem}}{M_{f,MD,HL}Cp}\left(Q_{h,HL} + Q_{N,HL}\right)\right] \tag{12}$$

$$\frac{\partial T_{f,MD,CL}}{\partial t} = -L_{MD}\left[\frac{m_{f,MD,CL}}{M_{f,MD,CL}}\frac{\partial T_{f,MD,CL}}{\partial x} - \frac{W_{mem}}{M_{f,MD,CL}Cp}Q_{h,CL}\right] \tag{13}$$

For each interface, the heat effects on both sides should be balanced.

$$\begin{aligned} &Q_{h,HL} + Q_{N,HL} - \Delta H_{VL,HL} = Q_{h,mem} + Q_{N,mem} = Q_{h,ag} + Q_{N,ag} \\ &= Q_{h,CONL} + Q_{N,CONL} - \Delta H_{VL,CONL} = Q_{h,cp} - \Delta H_{VL,CONL} = Q_{h,CL} - \Delta H_{VL,CONL} \end{aligned} \tag{14}$$

The heat fluxes of convective heat transfer, sensible heat transfer and latent heat transfer are determined by

$$Q_h = h\Delta T \tag{15}$$

$$Q_N = NCp\Delta T \tag{16}$$

$$\Delta H_{VL} = N\Delta H_{vap} \tag{17}$$

The heat transfer coefficients for hot fluid and cold fluid channels are estimated using the

correlation for laminar flow and constant wall heat flux (Holman 1989).

$$Nu = 4.36 + \frac{0.036\left[\frac{RePr}{L/D_h}\right]}{1 + 0.011\left[\frac{RePr}{L/D_h}\right]^{0.8}} \tag{18}$$

For the liquid film, the heat transfer coefficient is determined using the correlation for condensing film (Holman 1989).

$$h_{CONL} = 0.943\left[\frac{\rho_{CONL}(\rho_{CONL} - \rho_v)\Delta H_{vap} K_{CONL}}{L\mu_{CONL}(T_{CONL} - T_{mp})}\right] \tag{19}$$

For the membrane, air gap and cooling plate, the heat transfer coefficients are determined using the thermal conductivity and thickness of the layer. The membrane thermal conductivity is determined from the thermal conductivities of solid membrane and vapor inside the pore by using membrane porosity (ε) as the weighting factor.

$$h_{mem} = \frac{\varepsilon K_v + K_{mem}(1 - \varepsilon)}{\delta_{mem}} \tag{20}$$

$$h_{ag} = \frac{K_{ag}}{\delta_{ag}} \tag{21}$$

$$h_{cp} = \frac{K_{cp}}{\delta_{cp}} \tag{22}$$

The models are built on the commercial Aspen Custom Modeler® platform (Aspen Technology 2011) and solved using the built-in solver. The partial differential equations are transformed into differential algebraic equations using method of lines first and then solved by Newton's method. The models of AGMD, DCMD and VMD have been verified by experimental data (Meindersma *et al*. 2005, Chang *et al*. 2009, Hung 2014). In the previous study (Chang *et al*. 2012), the overall system model has been verified with a laboratory simulated SMDDS.

4. Equipment sizing

In this study, the s-SMDDS employing the flat sheet MD module developed and manufactured by the Swedish company Scarab AB are investigated. The module has been adopted in the solar desalination pilot plant of MEDESOL project (Guillén-Burrieza *et al*. 2011). Each module consists of 10 plastic cassettes with a total membrane area of 2.88 m^2. Although Scarab's module is of AGMD configuration, in this study, the membrane characteristics and dimensions of DCMD and VMD modules are assumed to the same as that of the Scarab's module with the modifications needed for different MD configurations. The attributions of the MD modules are summarized in Table 1. The three s-SMDDS systems analyzed are named AGMD, DCMD and VMD systems. For each of these systems, four MD modules are connected in series and the total membrane area is 11.5 m^2.

Table 1 Attributes of membrane module

Total membrane area (m^2)	2.8
Single sheet membrane width (m)	0.36
Single sheet membrane length (m)	0.39
Membrane material (porous+supporting)	PTFE+PP
Membrane thickness (μm)	30/170
Membrane pore diameter (μm)	0.2
Membrane porosity	0.8
Membrane tortuosity	1.33
Height of hot fluid channel (mm)	1
Height of cold fluid (mm) (for AGMD and DCMD)	1
Thickness of air gap (mm) (for AGMD)	1

Because of the intermittent and dynamic nature of the solar radiation, s-SMDDS is not operated under steady states. A pseudo steady state approach is proposed to determine the sizes of thermal storage tank, heat exchangers and circulation pump of loop 1. The concept is to view the s-SMDDS as a system operated at a pseudo steady state to transfer an amount of solar heat throughout the process, i.e., from the solar collector end to the MD unit end. The sizes of equipment units can then be determined based on the heat transfer rate and several specified variables, which are marked in red in Figs. 1-3 and discussed in the following.

The size of the thermal storage tank (V_{ST}) is determined by specifying the maximum temperature rise of the water in the tank over the maximum solar heat input period. For the solar collector with a specified area (A_{SC}) operated under the maximum solar radiation intensity ($I_{S\max}$) and the collector efficiency (η_{SC}), the maximum heat transfer rate ($q_{PS\max}$) from the solar collector to the thermal storage tank can be determined by

$$q_{PS\max} = A_{SC} I_{S\max} \eta_{SC} \tag{23}$$

In this study, the solar radiation profiles used, as shown in Fig. 5, are parabolic with different specified maximum intensity but the same day-time period of 11 hours. The solar collector efficiency is assumed to be 50% (Saffarini *et al*. 2012).

The energy balance for the water in the thermal storage tank over a time period of ($\Delta t_{\max}$) and a specified maximum temperature rise ($\Delta T_{S\max}$) of the water in the tank is given as

$$q_{PS\max} \Delta t_{\max} = \rho V_{ST} Cp(\Delta T_{S\max}) \tag{24}$$

The size of the circulation pump of loop 1 (F_{S1}) is determined using the maximum heat transfer rate and a specified temperature rise of loop 1 ($\Delta T_{Loop\,1}$) by

$$q_{PS\max} = F_{S1} Cp \Delta T_{Loop\,1} \tag{25}$$

The sizes of the heat exchangers (A_{HE}), including the single heat exchanger in AGMD system, the hot and cold heat exchangers in DCMD system and the hot heat exchanger and condenser in VMD system, are determined by the pseudo steady heat transfer rate (q_{PS}) in the heat exchanger

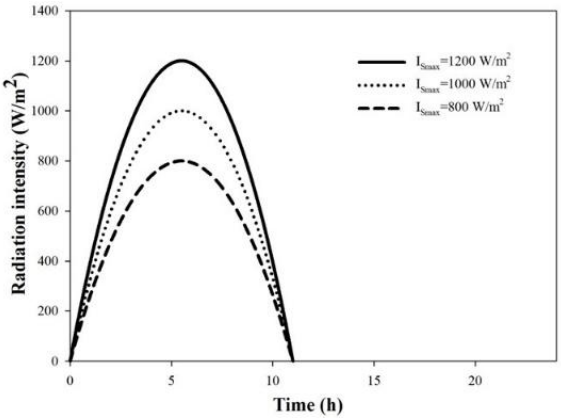

Fig. 5 Solar radiation profiles

with a specified logarithm mean temperature difference (ΔT_{lm}) and an assumed overall heat transfer coefficient (U_{HE}). Given the specified circulation flow rate of S3 (F_{S3}) and the temperature rise of loop 2 ($\Delta T_{Loop\,2}$), the pseudo steady heat transfer rate is calculated by

$$q_{PS} = F_{S3} Cp \Delta T_{loop\,2} \tag{26}$$

The area of each heat exchanger can then be calculated from the following design equation

$$q_{PS} = U_{HE} A_{HE} \Delta T_{lm} \tag{27}$$

The sizes of equipment units other than the thermal storage tank, pump 1 and heat exchangers are determined by dynamic optimization. In fact, they are the decision variables in the optimization problem.

5. Cost analysis

The capital, operating and total annual costs of the s-SMDDS are analyzed according to the following bases adopted by Banat and Jwaied (2008):

- The installation cost is 25% of the purchased cost of equipment.
- The instrumentation and control cost is 25% of the purchased cost of equipment.
- Zero land cost.
- Zero feed water pretreatment cost.
- Annual interest rate and plant lifetime for amortization of the capital cost or determining the annual fixed charge are 5% and 20 years, respectively.
- The annual operating and maintenance (O&M) cost is estimated to be 20% of the plant annual fixed charge.
- Membrane replacement rate is 20% per year.

The equipment costs are determined using the cost functions listed in Table 2. The cost function of solar collector with rack is based on the costs reported in Banat and Jwaied (2008) and has been adjusted with the CEPCI (Chemical Engineering Plant Cost Index) of 2013. The unit cost

Table 2 Cost functions of equipment units

Equipment	Purchased cost ($)	Notes
Solar collector	$C_{SC} = 890.78(A_{SC}/5.73)^{0.9}$	With rack.
Thermal storage tank	$C_S = 165(V_S/1000)^{0.57}$	Carbon steel.
Plate heat exchanger	$C_{HE} = [363.56 + 8.54\left(\frac{A_{HE}-1}{0.032}\right)]F_M$	$F_M = 3.5$ for anti-corrosion material of construction; $1\ m^2 \le A_{HE} \le 5\ m^2$.
Pump	$C_P = 265.4(F/95)^{0.4}F_M$	$F_M = 3.5$ for anti-corrosion material of construction; $F_M = 1$ for carbon steel; For a pumping head of 20 m.
Vacuum pump	$C_P = 340F_M$	$F_M = 1$ for carbon steel;
Membrane module	$C_{MD} = 410A_{mem}$	Flat sheet AGMD membrane module as the product from Scarab Development AB; PTFE membrane.

of membrane module is based on that used in Banat and Jwaied (2008) and MEDESOL project (2006) and is also adjusted with 2013 CEPCI. The cost functions of thermal storage tank, heat exchanger and pump are developed by this study based on the information provided by the equipment vendors. All the pumps are specified to provide a water head of 20 m. For the heat exchangers and the pumps for brackish or sea water, a material capital cost factor (F_M) is applied to account for the anti-corrosion material of construction used.

The unit cost of water production (c_w) is obtained from the total annual cost (TAC) of the system and the daily water production rate (F_{DW}) as given by

$$c_w = \frac{TAC}{F_{DW} \times 365} \tag{28}$$

The total annual cost is the sum of annual fixed charge (C_{fixed}), membrane replacement cost (C_{mr}), O&M ($C_{O\&M}$) and electricity costs (C_{elec}).

$$TAC = C_{fixed} + C_{mr} + C_{O\&M} + C_{elec} \tag{29}$$

The annual fixed charge can be calculated from the total purchased cost of all equipment units (C_{CC}) with the 25% installation cost and the amortization factor (a) as

$$C_{fixed} = a(1 + 25\%)C_{CC} \tag{30}$$

With the annual interest rate (i) and plant lifetime (n), the amortization factor is determined by

$$a = \frac{i(1+i)^n}{(1+i)^n - 1} \tag{31}$$

6. Dynamic optimization

Using the dynamic models of the s-SMDDS, the design of the system which gives the lowest unit cost for specified water production rate can be found out. Explained by the AGMD system, the optimization problem is defined as

$$\min(c_w) = f(A_{SC}, F_{S3}, F_{S8}, F_{S9}, F_{S11}) \tag{32}$$

Subject to:

- the desired distilled water production rate (F_{DW})
- solar radiation profile (I_S)
- parameters for pseudo steady state analysis - ΔT_{Smax}, ΔT_{lm}, $\Delta T_{Loop\,1}$, $\Delta T_{Loop\,2}$
- maximum temperature of S2 ($T_{S2} < 95^{o}\mathrm{C}$)

For each set of decision variables of the optimization problem, as specified in Eq. (32), the sizes of thermal storage tank, heat exchanger and pump 1 are determined by the methods explained in section 3. The flow rates of S3, S8, S9 and S11 are kept constant for the entire operation period. On the contrary, the flow rate of S1 is time-dependent. It is determined by the instantaneous solar heat input, the target temperature of S2 ($95^{o}\mathrm{C}$) and the temperature of S1

$$A_{SC} I_S \eta_{SC} = F_{S1} Cp(95 - T_{S1}) \tag{33}$$

It must be noted that although Eq. (33) is used to determine F_{S1}, the actual operation temperature of S2 will not reach $95^{o}\mathrm{C}$ as the results shown in section 7.3.

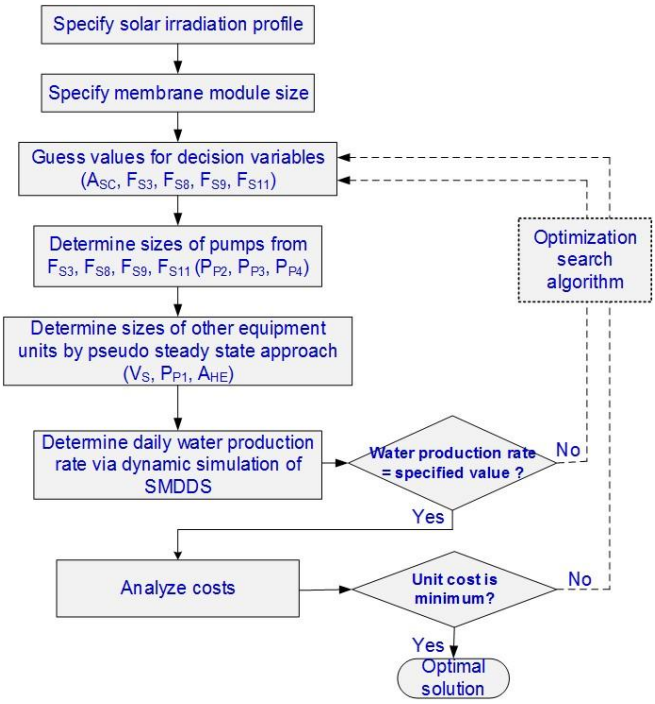

Fig. 6 The flowchart of the systematic optimization algorithm for AGMD system

The system operation will be stopped when the temperature of thermal storage tank is lower than $50^{o}C$.

For each of the AGMD, DCMD and VMD systems, this study implements the optimization analysis for different specified daily water production rates. The FEASOPT (Feasible Path Successive Quadratic Programming) algorithm built-in in the Aspen Custom Modeler® platform (Aspen Technology 2011) is adopted for the optimization search.

The systematic optimization algorithm for the AGMD system can be summarized by the flowchart shown in Fig. 6. The flowchart also applies to the DCMD and VMD systems, however, the variables should be changed.

7. Results and discussion

7.1 Optimal solutions and performance index

Because of the very high salt rejection capability of MD, in the case where potable water is required, the pure water product can be blended with raw water in order to obtain more potable water. In the previous economic evaluation studies (Banat and Jwaied 2008, MEDESOL project 2006, Saffarini *et al*. 2012), the unit cost with 1:1 dilution of the pure water produced is used for comparison with the production costs from other desalination technologies. In this study, the cost data presented is the 1:1 dilution cost, however, the water production rate is referred to the pure water produced from s-SMDDS. The 1:1 dilution cost is only used for comparison with literature data. It is not an assumption of the analysis and has no effects on the optimal design and cost results.

The minimum unit cost solutions for the AGMD system operated for daily water production rate of 100-600 kg/day are summarized in Table 3. The unit production costs ranged from \$5.92/m^3 to \$15.7/m^3. Both the equipment sizes and the circulation flow rates increase with the

Table 3 Optimal solutions for the AGMD system

F_{DW} (kg/day)	100	200	300	400	500	600
Performance index						
Unit cost with 1:1 dilution (\$/m^3)	15.70	8.54	6.55	6.01	5.92	7.05
STEC (kWh/m^3)	109.29	213.88	393.18	572.63	758.87	1424.76
PR	5.91	3.02	1.64	1.13	0.85	0.45
RR (%)	5.49	5.33	4.60	4.29	4.07	2.75
Decision variables						
A_{SC} (m^2)	1.36	5.35	14.76	28.70	47.57	107.21
V_{ST} (m^3)	0.07	0.28	0.76	1.48	2.46	5.54
A_{HE} (m^2)	1	1	1.01	1.66	2.55	2.97
F_{S3} (kg/h)	85.67	216.49	219.49	360.82	554.60	645.10
F_{S8} (kg/h)	0	0	0	0	0	0
F_{S9} (kg/h)	93.73	183.85	313.24	442.19	578.05	1015.95
F_{S11} (kg/h)	0	0	0	0	0	0

Table 4 Optimal solutions for the DCMD system

F_{DW} (kg/day)	100	200	300	400	500	600
Performance index						
Unit cost with 1:1 dilution ($/m^3)	19.43	12.43	10.60	9.81	9.44	9.48
STEC (kWh/m^3)	370.07	793.03	988.81	1149.58	1288.28	1418.17
PR	1.75	0.81	0.65	0.56	0.50	0.46
RR (%)	4.11	3.48	3.22	3.05	2.92	2.82
Decision variables						
A_{SC} (m^2)	4.60	19.82	37.14	57.61	80.76	106.72
V_{ST} (m^3)	0.24	1.02	1.92	2.98	4.17	5.51
$A_{H,HE}$ (m^2)	1	1.36	2.23	3.14	4.10	2.56
$A_{C,HE}$ (m^2)	1	1.36	2.23	3.14	4.10	2.56
F_{S3} (kg/h)	133.86	296.21	485.89	682.53	890.95	1112.62
F_{S6} (kg/h)	0	0	0	0	0	0
F_{S7} (kg/h)	114.50	267.38	432.13	608.64	792.58	985.46
F_{S10} (kg/h)	251.71	569.61	755.16	960.35	1197.15	1435.79
F_{S13} (kg/h)	0	0	0	0	0	0

Table 5 Optimal solutions for the VMD system

F_{DW} (kg/day)	100	200	300	400	500
Performance index					
Unit cost with 1:1 dilution ($/m^3)	22.08	12.90	10.83	10.25	10.41
STEC (kWh/m^3)	1595.69	1873.49	2363.43	2985.90	3790.95
PR	0.58	0.55	0.48	0.40	0.33
RR (%)	3.76	4.09	3.89	3.64	3.35
Decision variables					
A_{SC} (m^2)	13.83	29.17	50.31	80.10	121.90
V_{ST} (m^3)	0.75	1.51	2.60	4.14	6.30
A_{HE} (m^2)	1	1.05	1.65	2.35	3.18
A_C (m^2)	1	1.16	1.82	2.58	3.51
F_{S3} (kg/h)	316.00	457.48	813.05	1295.96	1965.84
F_{S7} (kg/h)	179.07	229.21	358.82	510.38	692.21
F_{S8} (kg/h)	0	0	0	0	0
F_{S9} (kg/h)	0	0	0	0	0

water production rate. In the optimization analysis, the minimum size of the heat exchanger is set to be 1 m^2. The lowest-cost case for the AGMD system is when 500 kg/day of pure water is produced with the solar collector area of 47.6 m^2 and the heat exchanger area of 2.55 m^2.

The minimum unit cost solutions for the DCMD system operated for daily water production rate of 100-600 kg/day are summarized in Table 4. The unit production costs fall between

$9.44/m^3$ and $19.43/m^3$, which are higher than that of the AGMD system. The lowest-cost case for the DCMD system is when 500 kg/day of pure water is produced with the solar collector area of 80.8 m^2 and area of 4.1 m^2 for both heat exchangers.

The minimum unit cost solutions for the VMD system operated for daily water production rate of 100-500 kg/day are summarized in Table 5. With the given size of MD module, water production rate of 600 kg/day cannot be obtained by the VMD system. The unit production costs fall between $10.25/m^3$ and $22.08/m^3$. The production cost of VMD system is the highest among the three systems. The lowest-cost case for the VMD system is when 400 kg/day of pure water is produced with the solar collector area of 80.1 m^2, heat exchanger area of 2.35 m^2 and condenser area of 2.58 m^2.

The variation of unit production cost with water production rate for the three systems are summarized in Fig. 7. With the given size of MD module, optimal production rate for each system can be obtained. For all the systems, the effect of production rate on unit cost becomes less significant when the production rate is at the high end, i.e., about 300 kg/day. The production cost of AGMD system is substantially lower than the other two systems for the entire range of production rate. On the other hand, the production costs of DCMD system and VMD system are fairly close.

The distribution of capital and operating costs of the lowest-cost AGMD, DCMD and VMD systems are presented in Fig. 8. For all the systems, the cost of solar collector contributes 39-45% of the total capital cost and is the highest among all equipment units. The second high capital cost equipment is the MD module for the AGMD system and the heat exchanger for the DCMD and VMD systems. For all the systems, the O&M cost is the highest operating cost item, which counts for 43-52% of the total operating cost. The second high operating cost item is the membrane replacement cost.

The equipment sizes and costs of the lowest-cost case, i.e., the AGMD system with 500 kg/m^3 production rate, are compared with the reported data for SMMDS from Banat and Jwaied (2008), MEDESOL project (2006) and Saffarini *et al.* (2012) in Table 6. The unit cost of the optimized AGMD system is about 1/3 of the costs reported in the cost evaluation literature.

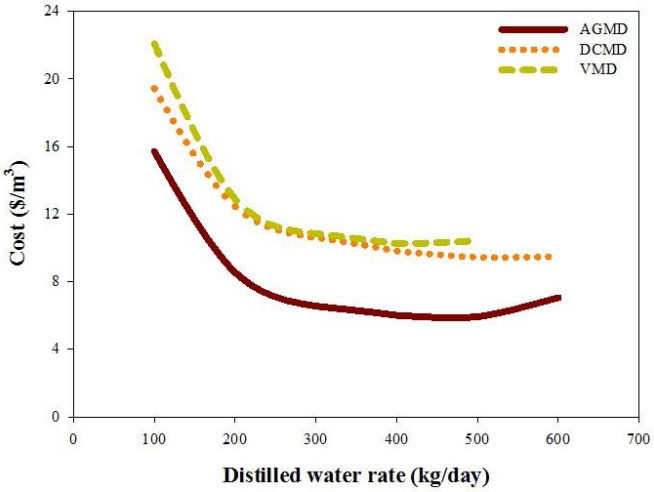

Fig. 7 Variation of unit production cost with water production rate

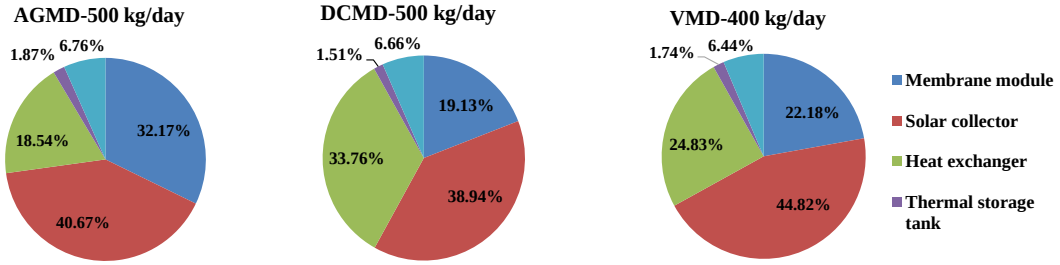

(a) Capital cost

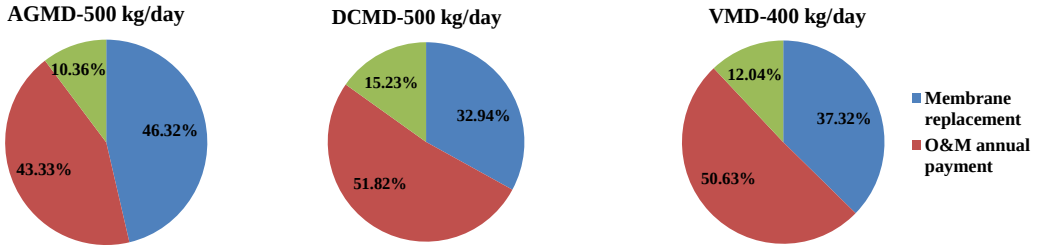

(b) Operating cost

Fig. 8 Comparison of capital and operating cost for optimal s-SMDDS using AGMD, DCMD and VMD

Table 6 Comparison of equipment sizes and cost data for SMDDS

Items	This study	Banat and Jwaied (2008) (compact/large)	MEDESOL (2006)[2]	Saffarini *et al.* (2012)
Capacity (kg/day)	500	100/500	73	700
Unit cost[1] ($/m^3)	5.92	15/18	15.67	18.26
Equipment size				
Membrane area (m^2)	11.5	10/40	2.3	7
Solar collector area (m^2)	47.57	5.73/72	2.6	N/A
Heat exchanger area (m^2)	2.55	0/N/A	$846	N/A
Thermal storage tank (m^3)	2.46	N/A	N/A	N/A
Cost data				
Membrane module	$4730	$1080/$4320	$808 ($360/m^2)	$350/m^2
Solar collector	$5985 w/ rack	$900/$8700 w/ rack	$385 ($150/m^2, w/o rack)	$160/m^2 (w/o rack)
Piping and tanks	$275	$200/$500	$62	$250
Heat exchanger	$2730	0/$1500	$846	$750
Pumps	$1000	$300/$700	$150	$700
Monitoring and control	3680	$3328/$10510	$385	$4500

* Notes: 1. Unit cost with 1:1 dilution;
2. The IC4 case - heat recovery at the cold side and performance ratio is 3.

For all the optimal solutions of the AGMD system, the flow rates of S8 and S11 are zero. These results reveal that: (1) the hot side recovery configuration is not beneficial to the overall system performance; and (2) the cold side recovery configuration should be operated by sending the entire cold side fluid out of the MD to the heat exchanger, i.e. without partial discharge. The MEDESOL project (2006) also concluded that the cold side recovery configuration is better. The same results are obtained for the DCMD and VMD systems and hence the same remarks on the heat recovery configuration can be made.

The reasons that the unit costs of the optimal systems designed in this study are much lower than the literature reported costs are:

- For the systems reported in the literature, the sizes of equipment units and operating conditions are either not rigorously determined or are determined by a steady state analysis with a constant solar radiation intensity.
- The systems reported in this study are designed via dynamic optimization. For the fixed membrane module sizes, all other equipment units are optimally sized. The flow rates of all the streams are also optimally determined, including the optimal time-varying flow rate of the solar collector circulation flow (S1). The flow rate of S1 varies with solar radiation and leads to higher temperature of the hot fluid in the MD module through the heat transfer via the thermal storage tank and the heat exchanger.

The desalination systems are commonly evaluated using several performance indexes, including PR (Performance Ratio, kg of water produced by the thermal energy of 1 kg steam), STEC (Specific thermal energy consumption, kWh/m^3) and RR (Recovery ratio, ratio of distillate rate to feed rate).

For the AGMD, DCMD and VMD systems, the effects of water production rate on PR are shown in Fig. 9. PR decreases with the increase of water production rate. Compared to the other two systems, the effect in the AGMD system is much drastic. If the AGMD system with the given membrane area of 11.5 m^2 were operated for very low water production rate, the PR value can be very high, however, it is in the expense of high unit production cost. The PR value corresponding to the lowest-cost case is 0.85. For the DCMD and VMD systems, the PR values are low and

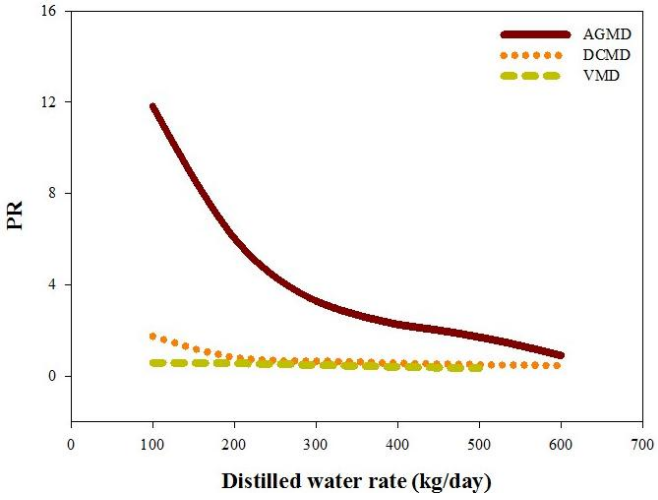

Fig. 9 Effects of water production rate on performance ratio

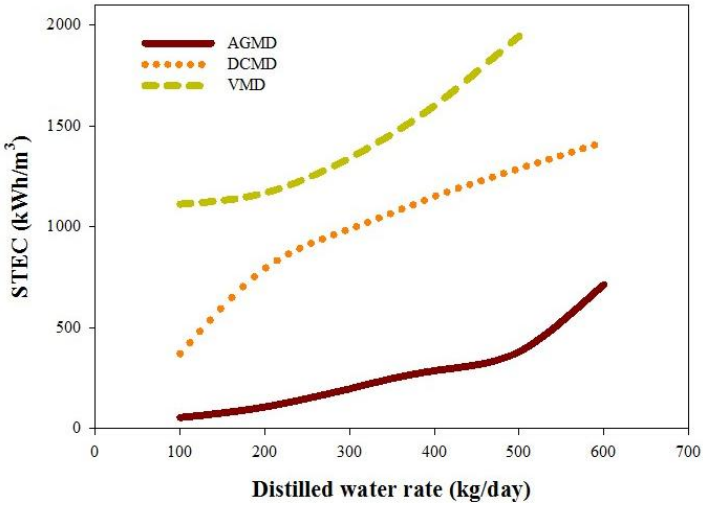

Fig. 10 Effects of water production rate on specific thermal energy consumption

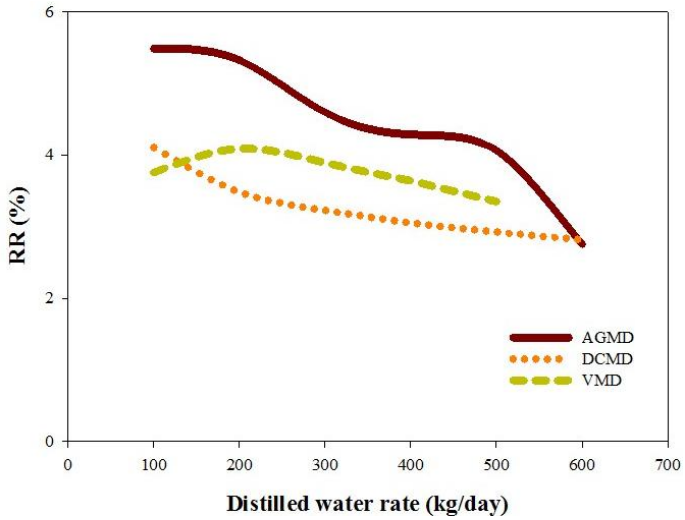

Fig. 11 Effects of water production rate on recovery ratio

insensitive to the water production rate. The results indicate that high PR value might not be a proper index to pursue for the design of s-SMDDS.

Since STEC and PR are counter performance indexes, the value of STEC increases with the water production rate as shown in Fig. 10. The AGMD system has the lowest STEC value. For the AGMD and DCMD systems, the value of RR decreases with the increase of water production rate as shown in Fig. 11. For the VMD system, the maximum value of RR corresponds to the 200 kg/day production. In Fig. 11, it shows that AGMD system operates at higher RR than the other two systems. However, when the production rate is high, the three systems approach the same RR value of about 2.8%. For the lowest-cost case, i.e. the AGMD system operated for 500 kg/day, RR is 4.07%. The case with the highest RR value is not the case with the lowest cost.

Table 7 Sensitivity analysis of pseudo steady state parameters of AGMD-500 kg/day system

$\Delta T_{S\max}$ (℃)	5	**10**	15
Unit cost ($/m^3)	7.74	**5.92**	5.12
$\Delta T_{HE,lm}$ (℃)	**5**	10	15
Unit cost ($/m^3)	**5.92**	5.77	5.71
$\Delta T_{Loop\,1}$ (℃)	15	**20**	25
Unit cost ($/m^3)	N/A	**5.92**	5.91
$\Delta T_{Loop\,2}$ (℃)	20	**25**	30
Unit cost ($/m^3)	5.82	**5.92**	6.03

* Notes: 1. Unit cost is with 1:1 dilution.
2. Bold face figures are base values. 3. N/A: the production rate of 500 kg/day cannot be obtained.

7.2 Sensitivity of pseudo steady state parameters

When employing the pseudo steady state approach, several parameters are specified, including $\Delta T_{S\max}$, ΔT_{lm}, $\Delta T_{Loop\,1}$ and $\Delta T_{Loop\,2}$. The effects of the values of these parameters should be examined. The sensitivity study is conducted by varying these parameters one by one from a set of base values, which are specified as 10℃, 5℃, 20℃ and 25℃ for $\Delta T_{S\max}$, ΔT_{lm}, $\Delta T_{Loop\,1}$ and $\Delta T_{Loop\,2}$, respectively. For the lowest-cost case of AGMD system, i.e. production rate of 500 kg/day, the sensitivity analysis results are listed in Table 7. The effects of these parameters are not significant except for very small $\Delta T_{S\max}$ and $\Delta T_{Loop\,1}$.

7.3 Operation performance of optimal systems

In this section, the daily operation performance of the lowest-cost s-SMDDS is presented. For the convenience of discussion, the optimal AGMD system with the lowest unit cost, i.e., 500 kg/day production rate, is called the AGMD-500 kg/day system. When operated under the solar radiation profile with $I_{S\max}$ equals to 1200 W/m^2, the daily operation profiles of AGMD-500 kg/day system are presented in Fig. 12. The solar collector operates for 9.5 hours, starting from the second hour after the sunrise. Other units, including thermal storage tank, heat exchanger and MD, operate for about 21 hours, starting from the third hour after the sunrise. The temperature profiles of all streams are shown in Fig. 12(a). The flow rate of pump 1 is determined by Eq. (25) and varies with time, which is different from other pumps with constant flow rates. The temperature profile of S2 is hence also different from that of those streams with constant flow rates. For all the heated streams, the profiles are dome shaped, but the profile of S2 has a longer high-temperature period. For all the heated streams, except S2, the time when the maximum temperature occurs is delayed from the time at the maximum solar radiation for about 5.5 hours. The maximum temperature of S2 is 83.7℃. The temperature differences between streams are greater when the stream temperatures are higher. The temperature of the discharged stream S7 falls between 31.8℃ and 35.9℃. It indicates that the heat recovery in the MD module is effective.

The flow rates of major streams, including S1, S3, S5, S7 and S9, are shown in Fig. 12(b). Because S8 is zero, S5 and S9 have the same flow rates. The flow rate of S7 is lower than that of S5 by the amount of flow rate of the distilled water S12 and fluctuates because of the time-varying production rate. The flow rate of S1 is varied according to Eq. (33) and has a maximum flow rate

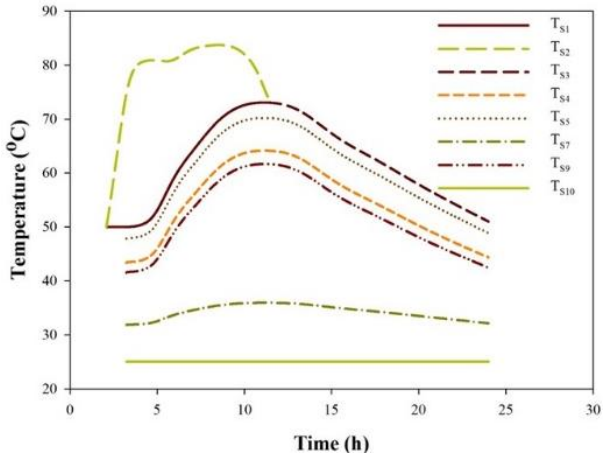

(a) Temperature

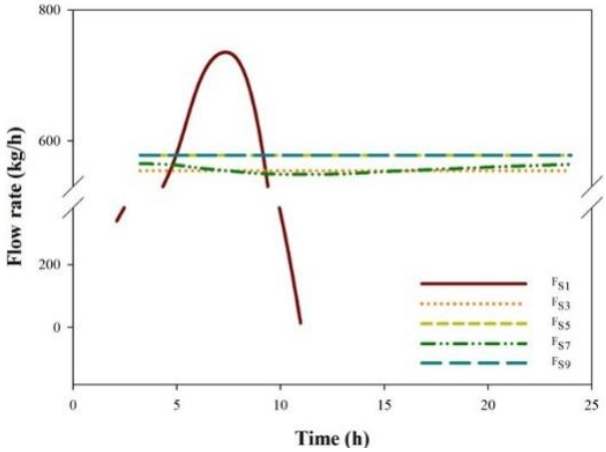

(b) Flow rate

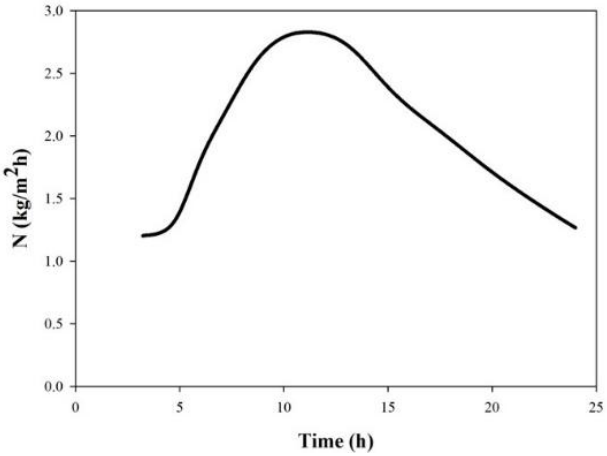

(c) Trans-membrane mass flux

Fig. 12 Operation profiles of AGMD-500 kg/day system for I_{max} = 1200 W/m^2

at about 1.8 hours after the maximum radiation time.

The trans-membrane mass flux profile is shown in Fig. 12(c). The flux is between 1.2-2.8 kg/m^{2}h. The time of maximum flux corresponds to that of the highest stream temperature. The trans-membrane mass fluxes of the lowest-cost DCMD and VMD systems range in 3.6-9.1 kg/m^{2}h and 3.1-9.3 kg/m^{2}h, respectively. Although the membrane fluxes are higher in the DCMD and VMD systems, the unit water production cost of the AGMD system is lower.

In order to understand how the optimal system which is designed for high-intensity solar radiation will perform under low-intensity solar radiation conditions, the AGMD-500 kg/day system is analyzed for the two solar radiation profiles with lower intensity as depicted in Fig. 5. For each solar radiation profile, the stream flow rates are optimized with the constraints of the maximum capacities of the equipment units and with the objective of maximizing daily water

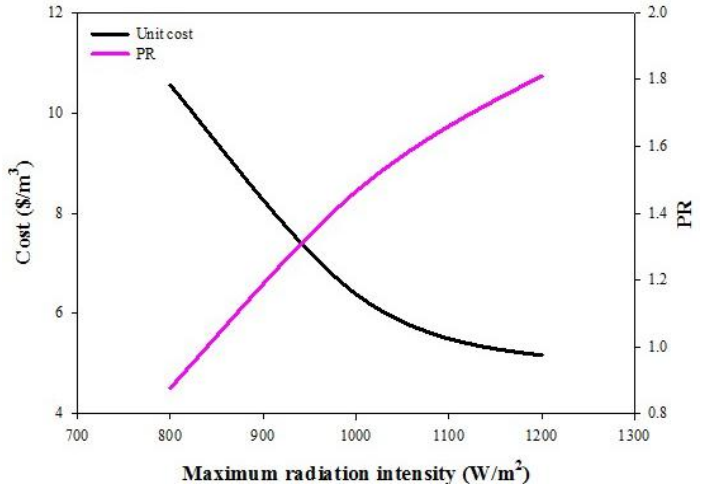

(a) Unit production cost and performance ratio

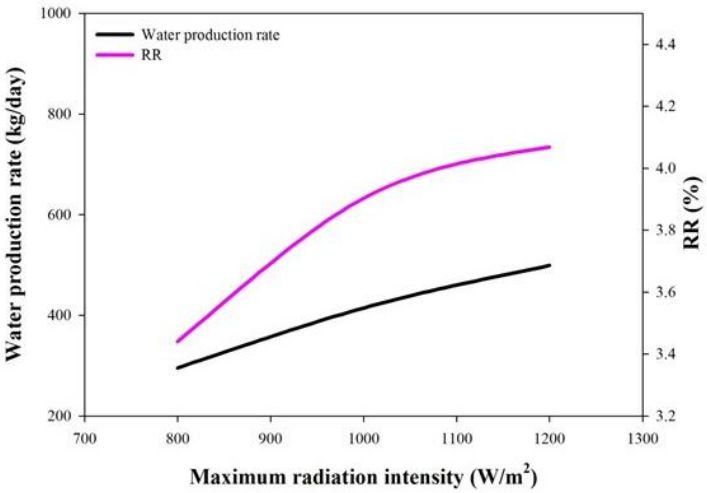

(b) Production rate and recovery ratio

Fig. 13 Effects of solar radiation intensity for AGMD-500 kg/day system

production rate. For the system with fixed equipment sizes, the effects of solar radiation intensity on the unit cost, PR, RR and water production rate are shown in Figs. 13(a) and (b). All these performance index decline with the decrease of solar radiation intensity.

7.4 Effect of membrane characteristics

The effect of enhancing membrane characteristics on the overall system performance can be easily investigated by enlarging the mass transfer coefficient or reducing the heat transfer coefficient of the membrane in the mathematic model. The results for AGMD-500 kg/day, DCMD-500 kg/day and VMD-400 kg/day systems are shown in Figs. 14 and 15. For these three systems, double the membrane mass transfer coefficient can result in the reduction of the unit cost

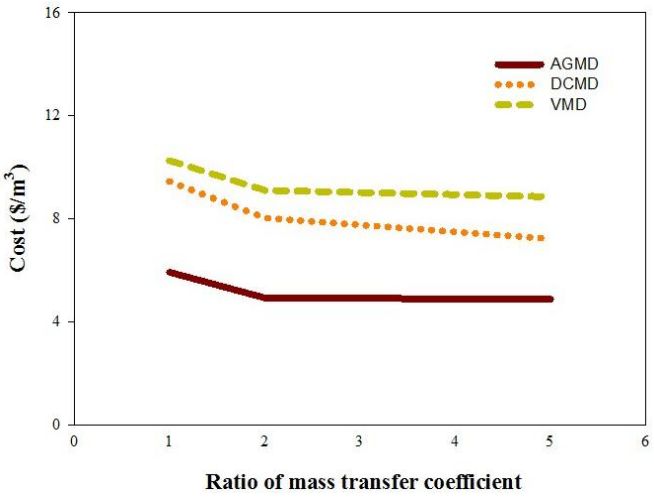

Fig. 14 Effects of membrane mass transfer coefficient on unit production cost

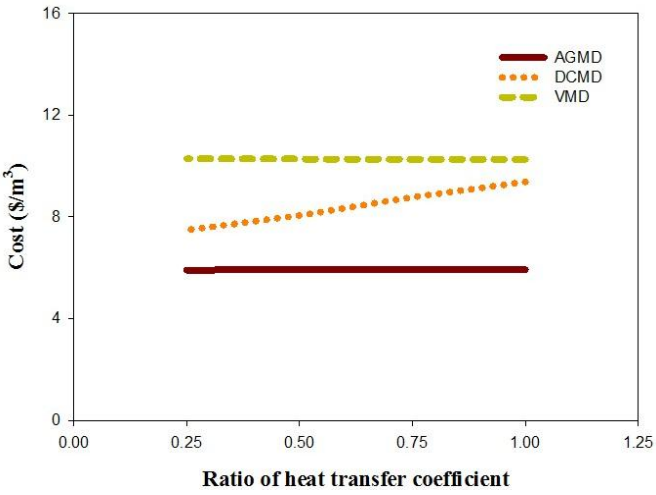

Fig. 15 Effects of membrane heat transfer coefficient on unit production cost

by 17%, 15% and 13%, respectively. However, the effects of further increase of the membrane mass transfer coefficient are relatively much smaller. Because of the difference in the heat transfer mechanism, only the reduction of membrane heat transfer coefficient of the DCMD system can result in the unit cost reduction and the effect is linear as shown in Fig. 15.

8. Conclusions

A systematic method for determining the optimal designs of s-SMDDS that produce water with minimum unit cost has been presented. The method utilizes a pseudo steady state approach for equipment sizing and the dynamic optimization analysis for taking into account the dynamic nature of the system.

Employing the systematic method, for a specified solar radiation profile, the optimal design of s-SMDDS using AGMD, DCMD and VMD with 11.5 m^2 of membrane area have been determined. The lowest-cost system uses AGMD and is operated for 500 kg/day water production rate. The unit cost for water production with 1:1 dilution is \$5.92/m^3, which is about 1/3 of the literature reported cost. The lowest-cost system does not correspond to the system with the highest performance ratio or recovery ratio.

For the membrane employed in this study, which is a common commercial product, the enhancement of membrane mass transfer coefficient for up to two times can result in the reduction of unit production cost of the system. The reduction of membrane heat transfer coefficient only affects the unit production cost of the DCMD system.

The results obtained from this study are limited to the flat sheet AGMD, DCMD and VMD modules with the specified MD sizes and cost functions employed. However, the approaches reported in this paper can be utilized to investigate the optimal design of SMDDS employing other MD configurations, such as liquid gap MD, as well as different membrane modules, such as spiral-wound and hollow fiber.

Acknowledgments

The authors gratefully acknowledge the sponsorship from the Ministry of Science and Technology of Taiwan.

References

Alkhudhiri, A., Darwish, N. and Hilal, N. (2012), "Membrane distillation: A comprehensive review", *Desalination*, **287**, 2-18.

Aspen Technology, Inc., MA, USA.

Banat, F. and Jwaied, N. (2008), "Economic evaluation of desalination by small-scale autonomous solar-powered membrane distillation units", *Desalination*, **220**(1-3), 566-573.

Camacho, L.M., Dumée, L., Zhang, J., Li, J.D., Duke, M., Gomez, J. and Gray, S. (2013), "Advances in membrane distillation for water desalination and purification applications", *Water*, **5**(1), 94-196.

Chang, H., Liau, J.S., Ho, C.D. and Wang, W.H. (2009), "Simulation of membrane distillation modules for desalination by developing user's model in Aspen Plus platform", *Desalination*, **249**(1), 380-387.

Chang, H., Wang, G.B., Chen, Y.H., Li, C.C. and Chang, C.L. (2010), "Modeling and optimization of a solar driven membrane distillation desalination system", *Renewable Energy*, **35**(12), 2714-2722.

Chang, H., Lyu, S.G., Tsai, C.M., Chen, Y.H., Cheng, T.W. and Chou, Y.H. (2012), "Experimental and simulation study of a solar thermal driven membrane distillation desalination process", *Desalination*, **286**, 400-411.

Chang, H., Chou, Y.H., Ho, C.D., Chang, C.L. and Chen, H.J. (2013), "Simulation study of desalination performance for two large-scale air gap membrane distillation modules", *Desalin. Water Treat.*, **51**(28-30), 5475-5484.

Ding, Z., Ma, R. and Fane, A.G. (2003), "A new model for mass transfer in direct contact membrane distillation", *Desalination*, **151**(3), 217-227.

Fath, H.E.S., Elsherbiny, S.M., Hassan, A.A., Rommel, M., Wieghaus, M., Koschikowski, J. and Vatansever, M. (2006), "PV and thermally driven small-scale, stand-alone desalination systems with very low maintenance needs", *Proceedings of the 10th International Water Technology Conference*, IWTC10 2006, Alexandria, Egypt, March, pp. 249-263.

Guillén-Burrieza, E., Blanco, J., Zaragoza, G., Alarcón, D., Palenzuela, P., Ibarra, M. and Gernjak, W. (2011), "Experimental analysis of an air gap membrane distillation solar desalination pilot system", *J. Membr. Sci.*, **379**(1-2), 386-396.

Holman, J. (1989), *Heat Transfer*, McGraw-Hill, New York, USA.

Hung, C.Y. (2014), "Optimal design of small-scale solar powered membrane distillation desalination systems", Master Thesis; Tamkang University, Taiwan.

Khayet, M. and Matsuura, T. (2011), *Membrane Distillation, Principles and Applications*, Elsevier, Amsterdam, Netherlands.

MEDESOL project (2006), "Performance and cost estimation of a standalone system based on MEDESOL technology", MEDESOL project Deliverable 14.
URL: http://www.psa.es/webeng/projects/medesol/documents/MEDESOL-DL14-CIE-UNAM-01.pdf

MEDESOL project website. URL: http://www.psa.es/webeng/projects/medesol/

Meindersma, G.W., Guijt, C.M. and de Haan, A.B. (2005), "Water recycling and desalination by air gap membrane distillation", *Environ. Progress*, **24**(4), 434-441.

Qtaishat, M.R. and Banat, F. (2013), "Desalination by solar powered membrane distillation systems", *Desalination*, **308**, 186-197.

Saffarini, R.B., Summers, E.K., Arafat, H.A. and Lienhard V, J.H. (2012), "Economic evaluation of stand-alone solar powered membrane distillation systems", *Desalination*, **299**, 55-62.

Summers, E.K., Arafat, H.A. and Lienhard V, J.H. (2012), "Energy efficiency comparison of single-stage membrane distillation (MD) desalination cycles in different configurations", *Desalination*, **290**, 54-66.

RJ

Symbols

A	Area (m^2)
a	Amortization factor
C_p	Heat capacity (J/kg K)
C	Cost ($ or $/year)
D_h	Hydraulic diameter (m)
D_m	Molecular diffusivity (m^2/s)
D_K	Kundsen diffusivity (m^2/s)
F	Flow rate (kg/h)
H	Height (m)
h	Heat transfer coefficient (W/m^2 K)
I	Intensity of solar radiation (W/m^2)
i	Interest rate
k	Mass transfer coefficient (m/s)
K	Thermal conductivity (W/m K)
L	Length of the equipment (m)
M	Mass of the fluid in the equipment (kg)
Mw	Molecular weight of water (kg/kmol)
m	Mass flow rate (kg/s)
N	Mole flux of water (kmol/m^2s)
Nu	Nusselt number
n	Plant life (years)
P	Pressure (Pa)
PR	Performance ratio (kg of water produced by the thermal energy of 1 kg steam)
Pr	Prandtl number
Q_h	Heat flux by convection or conduction (J/m^2s)
Q_N	Heat flux of the sensible heat transfer with the mass flux (J/m^2s)
q	Heat transfer rate (J/s)
R	Gas constant (Pa m^3/kmol K)
Re	Reynolds number
RR	Recovery ratio, ratio of distillate rate to feed rate
$STEC$	Specific thermal energy consumption (kWh/m^3)
T	Temperature (K)
TAC	Total annual cost ($/year)
t	Time
U	Overall heat transfer coefficient (W/m^2K)
V	Volume
W	Width of the equipment (m)
x	flow direction
y	mole fraction

Greek letters

ΔH_{VL}	Enthalpy for vapor-liquid phase change (J/m^{2}s)
ΔH_{vap}	Heat of vaporization (J/kmol)
ΔT	Temperature difference (K)
Δt	Time period (hour)
δ	Thickness (m)
ε	Porosity of the membrane
η	Collector efficiency
τ	Tortuosity of the membrane

Subscripts

ag	Air gap
air	Air
C	Condenser
CC	Capital cost
CL	Cold liquid
cp	Cooling plate
CONL	Considering liquid
DW	Distilled water
f	Fluid
fixed	Fixed
HE	Heat exchanger
HL	Hot liquid
lf	Liquid film
lm	Logarithmic mean
max	Maximum
MD	Membrane distillation
m1	Hot fluid-membrane interface
m2	Membrane-air gap interface
mem	Membrane
mr	Membrane replacement
O&M	Operating and maintenance
PS	Pseudo state
S	Solar
sat	Saturation
SC	Solar collector
ST	Thermal storage tank
v	Vapor
vap	Vapor
w	Water